Int. J. Electrochem. Sci., 11 **(2016)** 3767 - 3775

International Journal of
ELECTROCHEMICAL
SCIENCE
www.electrochemsci.org

Short Communication

The Thermoelectric Properties of Electrochemically Deposited Te-Sb-Bi Films on ITO Glass Substrate

Chao-Kai Yang[*], *Tsung-Chieh Cheng, Tao-Hsing Chen*[*], *Shih-Hua Chu*

Department of Mechanical Engineering, National Kaohsiung University of Applied Sciences, Kaohsiung 807, Taiwan
[*]E-mail: ck1114.yang@gmail.com; thchen@cc.kuas.edu.tw

Received: 15 January 2016 / *Accepted:* 29 February 2016 / *Published:* 1 April 2016

In this study, we use ITO glass to deposit thermoelectric thin films by using electrochemically deposition method. With electrochemical deposition, we deposit Te-Bi-Sb thin films on ITO glasses, trying to probe into different influences on thermoelectric characteristics by changing Sb^{3+} consistency and current density. The finished Te-Bi-Sb thin films will be observed by Scanning Electron Microscope (SEM) to realize the microstructure, also, be identified the crystal structure with XRD, and electrical analysis. The result finds out the thin film is a P-type thermoelectric material. Owing to the variation of current density or electrolyte density affects and changes the structure of Te-Bi-Sb film, the study categorizes three types of forming structures: Ball-type, Mixed-type, and Acicular-type; the ion content of the precipitated film can be controlled by alter current or electrolyte density. Good thermoelectric material requires high Seebeck coefficient, and the best one in the study is in the condition of 38mM-2.1mA/cm^2, which results in 32.89μV/K. Also, power factor is a criterion to evaluate a material, and bigger factor equals to better quality. In this study, we get the best power factor in the condition of 15mM-2.1 mA/cm^2, with the result of 49.5505α^2/ρ.

Keywords: Electrodeposition, Thermoelectric thin film, Seebeck

1. INTRODUCTION

With the growing cost of energy and increasingly serious global warming, it has become vitally important to find clean and sustainable energy resources. Thermoelectric (TE) conversion technology has drawn some serious attention because it can be used to convert waste heat to usable electricity with a subsequent improvement in energy efficiency. Electric and electronic devices are becoming smaller and lighter with every new model released. The components, such as Integrated Circuits (IC) are smaller and closer together and this dense concentration of parts emits quite a lot of thermal power.

doi: 10.20964/110371

This localized heat can influence the function and properties of electrical parts and so it is necessary that it be removed. Doing this by thermoelectric cooling of the ICs can quickly remove the heat, is quiet and efficient and conforms to current environmental protection thinking. Previous work [1-6] has been done where Films, Nanowires and Superlattices have been used to make Low-dimensional scale thermoelectric material. However, the ZT of these materials can certainly be improved [7].

Recently, Venkatasubramanian et al, at the Rochester Institute of Technology (RIT) in the US, used Molecular Beam Epitaxy (MBE) to grow Bi_2Te_3/Sb_2Te_3 Super Lattice nanowire films, and the energy of the Band Gap of the material under the quantum effect was raised. Furthermore, the interface of multi-layer Super Lattice film can add extra scattering probability of heat conducting phonons, so the ZT value of these Bi_2Te_3/Sb_2Te_3 films was initially estimated to be more than 2 [8]. Since the electrical and electronic components used in different devices generate different amounts of heat, different thermoelectric material is indicated according to the temperature and application. These thermoelectric materials can be divided into three types [9]: 1) Bi-Te alloys which can be used at room temperature, usually used in thermoelectric cooler. 2) Pb-Te alloys are used at temperatures around 400K. 3) Si-Ge alloy are useful at temperatures above 800K, and Pb-Te and Si-Ge alloys are primarily used in thermoelectric generator. Bi-Te-Sb is a P type thermoelectric material [9] that can be used at room temperatures. These thermoelectric films can be produced by many techniques, such as sputtering [10], metal organic chemical vapor deposition (MOCVD) [11], arc melting furnace [12], evaporation [13] and electrochemical deposition [14].

Electrochemical deposition is a low-cost method that can be used to grow high-quality metal, alloy and semiconductor films [15-20]. Many researchers have also tried to use electrodeposition methods to deposit Te-Bi nanowire thermoelectric material on anodic aluminum oxide (AAO) [21, 22]. Li and Miyazaki et al [23, 24] used Au and Pt as the substrate, but the cost of thermoelectric material made with Au and Pt was rather high. In our work we used indium tin oxide (ITO) as the substrate. This material has high light transmission and low resistance and several electrochemical deposition methods were explored for making Bi_2Te_3 thermoelectric film on ITO substrate.

2. EXPERIMENTAL AND MATERIALS PREPARATION

2.1. Experiment materials

High-purity chemical grade Bi_2O_3, TeO_2 and Sb_2O_3 were used in this work and the solvents used were saltpeter (KNO_3), tartaric acid and perchloric acid solutions respectively. Te-Bi-Sb films were deposited on ITO glass substrates using platinum titanium mesh as the positive pole.

2.2 Preparation of test pieces

The ITO glass to be used as substrate was cleaned thoroughly in deionized water, ethyl alcohol and acetone and then dried in a stream of nitrogen gas before being cut into $18\times18cm^2$ pieces to be used in the experiments.

The two variables in these experiments were the concentration of the Sb_2O_3 used, 15mM, 24mM, 38mM and the electroplating current density, 1.1mA/cm^2, 1.5mA/cm^2, 2.1mA/cm^2. The solutions used in the process: 2mM TeO_2 and 0.5mMBi_2O_3 were dissolved by magnet with stirring in 1MHNO_3 solution, 3.5M$HClO_4$ solution and 0.35M$C_4H_6O_6$ solution respectively. Calculations of the solution concentrations and the current density to be used were made before the electroplating work was done. The volume of electroplating solution used was 100mL and platinum titanium mesh was used as the Anode. The test piece was placed at a fixed distance from the anode and the solution was both aerated and stirred (magnetic stirrer) constantly to remove the hydrogen bubbles generated by the process and ensure an even distribution of metal ions. The supply voltage was monitored by a Keithley 2410 multi-function power meter and the plating time was 45 minutes. The test pieces were taken from the bath, cleaned in deionized water and dried in a stream of nitrogen gas before being examined.

2.3 Structural analysis and observation

The surface structure of the Te-Bi-S thermoelectric film on the test pieces was examined by scanning electron microscopy (SEM) and by X-Ray diffraction (XRD) to analyze and identify the crystal phase of the films and determine their physical nature on the different test pieces.

2.4. Electrical analysis

A four-point probe was used to determine the film resistivity under various conditions, and the Seebeck coefficient was measured using a self-made Seebeck measuring instrument. Sheet resistance is one of the importance characteristics of conductive materials and can be influenced by film thickness, grain size, grain structure, impurity and doping concentration and alloy composition. The Four-Point Probe is the most commonly used tool to measure sheet resistivity. A fixed current is applied between two points and the voltage difference between two other points is measured to allow the sheet resistivity to be calculated. If the thickness is much smaller than the current diffusion depth (t<<S), the relationship between resistance and voltage and current can be expressed by the following formula

$$\rho = \frac{V}{I} \cdot t \cdot \frac{\pi}{\ln 2} \quad (1)$$

The Seebeck coefficient was determined by subjecting the test blocks to different temperatures and measuring voltage differences using a Keithley 2410 multi-function power meter. The temperatures were measured using a T-type thermoelectric couple connected to a temperature measuring device (mv100 mobile Coder). The range of temperatures that could be measured by this device was between -10°C and 150°C. Points were recorded at 1°C intervals, and the values were used to calculate the Seebeck coefficient using the formula below:

$SAB = SB - SA = V / \Delta T$

3. RESULTS AND DISCUSSION

3.1 The Bi-Te-Sb film growth mechanism

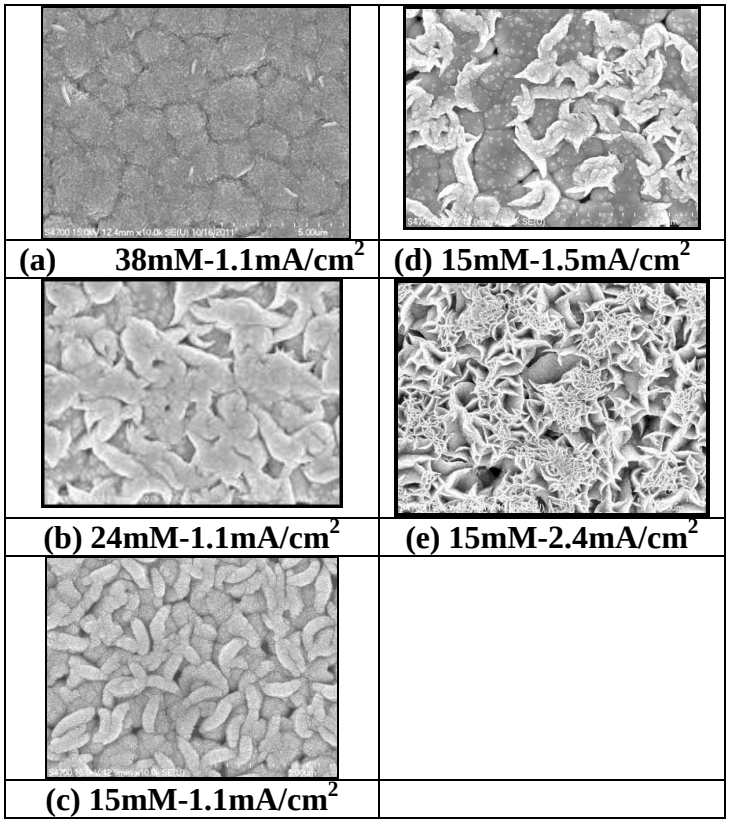

Figure 1. SEM images of the three types of Te-Bi-Sb film structure: (a) ball, (b) comprehensive, and (c) acicular, (d) acicular, (e) acicular.

The characteristics of thin film, such as crystal structure and mechanical strength, are determined by the growth mechanism. XRD and SEM can be used to determine crystal microstructure, phase changes, the presence of impurities, or any anomaly arising during the process of deposition and growth. The XRD diffraction pattern can be compared with the JCPDS-ICDD card number to define the film crystal structure.

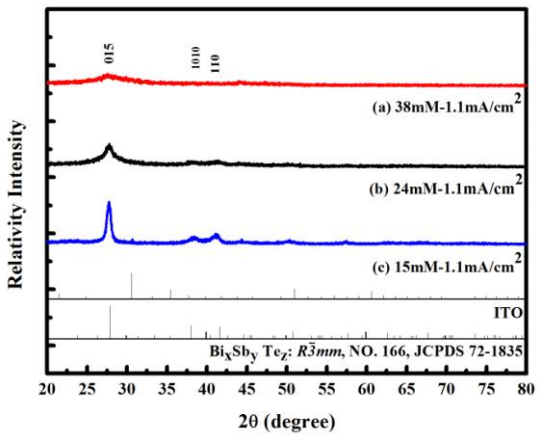

(a)

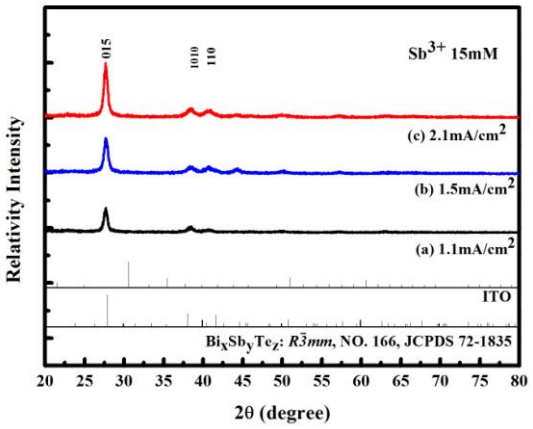

(b)

Figure 2. XRD pattern of the Te-Bi-Sb film (a) under the same current density, (b) under the same Sb+3 concentration.

Figure 1 shows SEM images of the three types of Te-Bi-Sb film structure obtained in these experiments. From these figures, the acicular is the best structure. It can be investigated further in the XRD analysis.

From the XRD diffraction pattern of the three Te-Bi-Sb film structures (Figure 2(a)), we can see that the plane diffraction intensity (015) is the strongest and this is preferred growth direction. It is also easy to see that the ball crystal structure is not good and the best structure is clearly acicular.

Comparing the electrochemical condition Fig. 1(a) to Fig. 1(c), they are under the same current density but different Sb3+ concentration. It can be identify the film quality from Fig. 2(a). Due to the specimen of Fig. 1(c) has higher peak value than specimens of Fig. 1(a) and Fig. 1(b). It can be known the poor crystals in the ball structure with high Sb3+ concentration. However, we compare the same Sb3+ concentration but different current density (see Fig. 1(c) to Fig. 1(e)). The higher current density has good crystal structure due to the high XRD peak value (shown in Fig. 2(b)). The reason for the better acicular crystallinity is the current density which causes rapid grain growth to give better crystals[25, 26]. The reason for the poor crystals in the ball structure was high Sb^{3+} concentration. Bi and Te both have a rhombohedral crystal lattice, but Sb is cubic. The difference in lattice form leads to a pileup of incompatible material which results in very poor crystallinity. This has also been observed by Li and Wang et al [27, 28]. Our XRD observations and JCPD comparison shows that the thermoelectric films made in this study have rhombohedral surface lattice. And it is also clearly shown that an increase in Sb content causes the crystallinity of the film to deteriorate.

3.2. Thermoelectric property analysis

The resistivity analysis of Te-Bi-Sb films under different Sb+3 concentration and current density, which is shown in Fig. 3. It can be seen that for any particular concentration of Sb^{3+}, the higher the current density, the greater the resistivity. In higher Sb^{3+}concentration, it has the highest resistivity. It can be confirmed that under higher Sb+3 concentrations, it has poor crystal structure and poor growth of film. Under the same Sb+3 concentrations, the resistivity increases slowly with

increasing current density. In other words, with a fixed Sb^{3+} concentration, an increase in current density will cause faster grain growth. This leads to an increase of inner stress, and inner stress results in crystal structure deformation. The acicular structure becomes blooming flower and structural porosity increases, it is reason for the current density increases with increasing resistivity under the same Sb+3 concentration. But for a fixed current density, the higher the Sb^{3+} concentration, the greater the likelihood of Sb^{3+} entering the film and this makes the microstructure flatter and crystallinity is poor. Electron mobility is poor due to interference from grain boundaries and will results in the increasing of resistivity. The increase of current density or Sb^{3+} concentration can also make grains grow faster. Acicular structure has poor electron mobility and increases the resistivity [29, 30].

Figure 4 is the relationship diagram between the Seebeck coefficient of Te-Bi-Sb film and current density. From these figure it can be seen that the Seebeck coefficient is positive because the thermoelectric material used in this study was P type. Under the same Sb^{3+} concentration, the Seebeck coefficient will increase with an increasing current density. With a fixed current density the influence of Sb^{3+} concentration on the Seebeck coefficient is not great. The best Seebeck coefficient is 32.89μV/K which was obtained with 38mM-2.1mA/cm^2.

The power factor properties of Te-Bi-Sb films with different current density is shown in Figure 5. From the figure, we can see that for a particular current density, the power factor drops with an increase in Sb^{3+} concentration. Experiments with the same Sb^{3+} concentration, show that the power factor increases with a increasing current density. The best power factor is 49.5505α^2/ρ which was obtained in the experiment using 15mM-2.1 mA/cm^2. Since the power factor is defined by α^2/ρ, α being the Seebeck coefficient and ρ resistivity, the resistivity clearly increases with an increasing Sb^{3+} concentration. This means the power factor decreases with the increasing Sb^{3+} concentration. Also, since the increase of current density or Sb^{3+} concentration can make the grains grow faster, a defective structure can easily occur in this process and cause an increase of resistivity and a decrease of the power factor. This greater power factor is attributed to the significant mainly increase in the electrical conductivity without any mainly significant decrease in the Seebeck coefficient. So the best thermoelectric property is the condition of 15mM-2.1 mA/cm^2. It also can be known the current density is the important factor when deposited the Bi-Te-Sb thermoelectric thin film in the ITO substrate [31, 32].

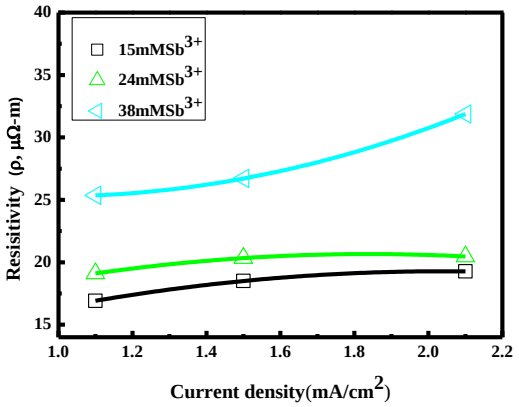

Figure 3. Relationship diagram between resistivity of Te-Bi-Sb film and current density.

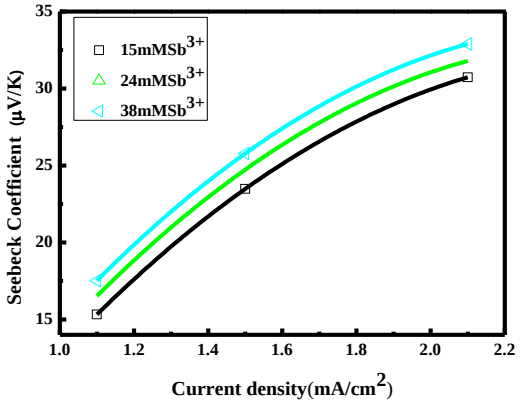

Figure 4. Relationship between Seebeck coefficient of Te-Bi-Sb film and current density.

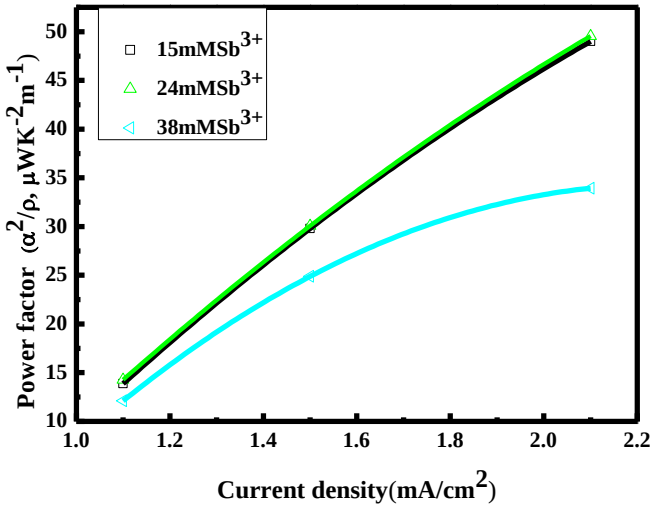

Figure 5. Relationship between the power factor of Te-Bi-Sb film and current density.

4. CONCLUSION

In this study Bi_2O_3, TeO_2 and Sb_2O_3, were dissolved in saltpeter (KNO_3), tartaric acid solution and perchloric acid solution and used for the electrochemical deposition of Te-Bi-Sb films on ITO glass substrates at room temperature. The study included an analysis of Bi-Te-Sb film structure and thermoelectric properties and of the results of processing at different current density and Sb^{3+} concentration. The conclusions reached were:

1. The Bi-Te-Sb film made in this study was P type thermoelectric material.
2. The change of current density and electrolyte solution concentration can cause changes in the structural form of the resulting electrodeposited Bi-Te-Sb film. Three types of crystalline structure were produced (ball, comprehensive and acicular).
3. The best Seebeck coefficient of deposited Bi-Te-Sb was 32.89μV/K which was gained under experimental conditions using 38mM-2.1mA/cm^2. The best power factor was 49.5505α^2/ρ which was achieved using 15mM-2.1 mA/cm^2.

ACKNOWLEDGEMENTS
This work was supported and funded under Project No. NSC 101-2221-E-151-010 and 102-2212-E-151-006-MY3 of the National Science Council (NSC) for which the authors extend their most sincere gratitude.

References

1. G.J. Snyder, J.R. Lim, C.K. Huang and J.P. Fleurial, *Nat. Mater.*, 2 (2003) 258.
2. A. I. Boukai, Y. Bunimovich, J. Tahir-Kheli, J. K. Yu, W. A. III Goddard and J. R. Heath, *Nat. Mater.*, 451 (2008) 168.
3. L. D. Hicks and M. S. Dresselhaus, *Phys. Rev. B*, 47 (1993) 12727.
4. Y. M. Lin and M. S. Dresselhaus, *Phys. Rev. B*, 68 (2003) 075304.
5. G. Chen, *Phys. Rev. B*, 57 (1998), 14958.
6. D.Y. Chung, T. Hogan, P. Brazis, M. Rocci-Lane, C. Kannewurf, M. Bastea, C. Uher and M.G. Kanatzidis, *Science*, 287 (2000) 1024.
7. A. Majumdar, *Science*, 303 (2004) 777.
8. M.K. Han, K. Hoang, H.J. Kong, R. Pcionek, C. Uher, K.M. Paraskevopoulos, S.D. Mahanti and M.G. Kanatzidis, *Chem Mater*, 20 (2008) 3512.
9. T.M. Tritt, *Science*, 283 (1999) 804.
10. D.H. Kim, E. Byon, G.H. Lee and S. Cho, *Thin Solid Films*, 510 (2006)148.
11. A. Giani, A. Boulouz, F. Pascal-Delannoy, A. Foucaran and A. Boyer, *Thin Solid Films*, 315 (1998) 99.
12. T.H. Chen and M.T. Hong, *Int. J. Electrochem. Sci.*, 10 (2015) 9417.
13. J. Dheepa, R. Sathyamoorthy and A. Subbarayan, *J. Cryst. Growth*, 274 (2005) 100.
14. K. Tittes, A. Bund, W. Plieth, A. Bentien, S. Paschen, M. Plötner, H. Gräfe and W. J. Fischer, *J. Solid State Electrochem.*, 7 (2003) 714.
15. R. Venkatasubramanian, T. Colpitts, E. Watko, M. Lamvik and N. El-Masry, *J. Cryst. Growth*, 170 (1997) 817
16. O. Bubnova, M. Berggren, and Xavier C., *J. Am. Chem. Soc.*, 134 (2012) 16456.
17. H. Shi, C. Liu, J. Xu, H Song, Q Jiang, B Lu, W Zhou and F Jiang, *Int. J. Electrochem. Sci.*, 9 (2014) 7629.
18. Y. Ma, E. Ahlberg, Y. Sun, B. B. Iversen, Anders E.C. Palmqvist, *Electrochim. Acta*, 56 (2011) 4216.
19. M. Abellán, R. Schrebler and H. Gómez, *Int. J. Electrochem. Sci.*, 10 (2015) 7409.
20. Y. Ma, E. Ahlberg, Y. Sun, B. B. Iversen and Anders E. C. Palmqvista, *J. Electrochem. Soc.*, 159 (2012) D50
21. H. Xu and W. Wang, *Int. J. Electrochem. Sci.*, 8 (2013) 6686.
22. J. Lee, S. Farhangfar, J. Lee, L. Cagnon, R. Scholz, U. Gösele and K. Nielsch, *Nanotechnology*, 19 (2008), 365701.
23. F. Li and W. Wang, *Appl. Surf. Sci.*, 255 (2009) 422.
24. Y. Miyazaki and T. Kajitani, *J. Cryst. Growth*, 229 (2001) 542.
25. R. Yamada, H. Wano, K. Uosaki, *Langmuir*, 16 (2000) 5523.
26. F. H. Li, F. L. Jia, W. Wang, Appl. Surf. Sci. 255 (2009) 7394
27. F. Li and W Wang, *Electrochim. Acta*, 54 (2009) 3745.
28. F. Li, and W. Wang, *Electrochim. Acta*, 55 (2010) 5000.
29. S.K. Lim, M.Y. Kim and T.S. Oh, *Thin Solid Films*, 517 (2009) 4199.
30. M. Takashiri, K. Miyazaki, S. Tanaka, J. Kurosaki, D. Nagai and H. Tsukamoto, *J. Appl. Phys.* 104 (2008) 84302.
31. C.L. Wan, Y.F. Wang, N. Wang and K. Koumoto, *Materials* 3 (2010) 2606.

32. L. Su and Y. X. Gan, *Electrochim. Acta*, 56 (2011) 5794.